SANDIA REPORT
SAND2000-0958
Unlimited Release
Printed April 2000

Using Rigid Polyurethane Foams (RPF) for Explosive Blast Energy Absorption in Applications Such as Anti-Terriorist Defenses

Ronald L. Woodfin

Prepared by
Sandia National Laboratories
Albuquerque, New Mexico 87185 and Livermore, California 94550

Sandia is a multiprogram laboratory operated by Sandia Corporation, a Lockheed Martin Company, for the United States Department of Energy under Contract DE-AC04-94AL85000.

Approved for public release; further dissemination unlimited.

Sandia National Laboratories

Issued by Sandia National Laboratories, operated for the United States Department of Energy by Sandia Corporation.

NOTICE: This report was prepared as an account of work sponsored by an agency of the United States Government. Neither the United States Government, nor any agency thereof, nor any of their employees, nor any of their contractors, subcontractors, or their employees, make any warranty, express or implied, or assume any legal liability or responsibility for the accuracy, completeness, or usefulness of any information, apparatus, product, or process disclosed, or represent that its use would not infringe privately owned rights. Reference herein to any specific commercial product, process, or service by trade name, trademark, manufacturer, or otherwise, does not necessarily constitute or imply its endorsement, recommendation, or favoring by the United States Government, any agency thereof, or any of their contractors or subcontractors. The views and opinions expressed herein do not necessarily state or reflect those of the United States Government, any agency thereof, or any of their contractors.

Printed in the United States of America. This report has been reproduced directly from the best available copy.

Available to DOE and DOE contractors from
Office of Scientific and Technical Information
P.O. Box 62
Oak Ridge, TN 37831

Prices available from (703) 605-6000
Web site: http://www.ntis.gov/ordering.htm

Available to the public from
National Technical Information Service
U.S. Department of Commerce
5285 Port Royal Rd
Springfield, VA 22161

SAND2000-0958
Unlimited Release
Printed April 2000

Using Rigid Polyurethane Foams (RPF) for Explosive Blast Energy Absorption in Applications Such as Anti-Terrorist Defenses

Ronald L. Woodfin
Explosive Subsystems and Materials Department
Sandia National Laboratories
P. O. Box 5800
Albuquerque, NM 87185-1452

Abstract

Reduction of the data from recent experiments has shown that RPFs have a remarkable and surprising capability to absorb and perhaps to dissipate the energy of a blast wave. The actual energy absorbing mechanisms seem quite complex. There is, in spite of the lack of fundamental understanding of mechanisms, a potential to use this material as a protective measure in a number of situations. The possibility of ship hull protection has been considered. Another possibility is the protection of concrete structures from a terrorist attack, such as a satchel charge placed in contact, or a larger charge placed some distance away. The purpose of this report is to document the recent work done to quantify the blast energy absorbing capability of the RPF material as well as possible from the existing data, and to suggest appropriate avenues for research to gain better definition of the mechanisms involved. In addition, some potential applications are suggested. All of the data presented herein are digested from the earlier reports. This report only considers analysis of those data. Details of the experiments and techniques that produced the data are in those reports. RPF can form a valuable tool in protecting structures against blast, such as from terrorist attack. Experiments are needed to confirm the predictive capability of the derived extrapolator. These experiments are needed to make intelligent design decisions, but, as an interim, a nine-inch thick layer of six-to-eight pound per cubic foot (pcf) RPF can be considered sufficient to greatly reduce damage, especially interior spalling, from concrete walls in a variety of attack scenarios. A six-inch thick layer is almost as effective. This analysis has considered only blast wave damage. RPF should not be used for protection against explosively driven fragments. This analysis does not consider the effect of the pressure pulse on the overall structure.

Intentionally Left Blank

Contents

Background 6
Introduction 7
Available Data 7
Analysis of Cavity Formation Data 11
Analysis of Flyer Plate Data 14
Adjustment for Density and Explosive Used: 19
Extrapolation to Larger Explosive Charges 21
Investigation of Reduction in Ground Crater Size by RPF Layer 28
Conclusion 29

Figures

Figure 1. RPF Destroyed in a Variety of Experiments 8
Figure 2. Data from Explosive Tests on Foams (replotted from Cooper & Kurowski, October 6, 1975) 9
Figure 3. Data from fully Embedded Explosive Tests on Foams (replotted from Cooper & Kurowski, October 6, 1975) 10
Figure 4. Diagram of Flyer Plate Apparatus (See Reference 2 for More Details) 11
Figure 5. Cavity Diameters Produced in RPF by Tetryl and TNT Unit Charges (from Cooper & Kurowski Formula) 12
Figure 6. Mass of RPF Destroyed by Tetryl & TNT Unit Charges (from Cooper & Kurowski formula) 13
Figure 7. Flyer Plate Velocity Attenuation by 5.7 pcf (RPF 14
Figure 8. Incremental Energy Density Absorbed in 5.7 pcf RPF layers 15
Figure 9. Cumulative Energy Density in 5.7 pcf RPF from PETN Plate Charge 16
Figure 10. Total Energy Absorbed by 5.7 pcf RPF 17
Figure 11. Total Specific Energy Absorbed by 5.7 pcf RPF 18
Figure 12. Total Absorbed Specific Energy Density of 5.7 pcf RPF 19
Figure 13. Absorbed Energy Density in 5.7 pcf RPF from PETN Plate Charges 20
Figure 14. Specific Energy Density Absorbed from PETN Plate Charges in 5.7 pcf RPF 21
Figure 15. Energy Flux Absorbed by 5.7 pcf RPF from PETN Plate Charges 22
Figure 16. Specific Energy Flux Absorbed in 5.7 pcf RPF by PETN Plate Charges 23
Figure 17. Energy Density Flux Absorbed in 5.7 pcf RPF from PETN Plate Charge 24
Figure 18. Specific Energy Density Flux Absorbed in 5.7 pcf RPF from PETN Plate Charges 25
Figure 19. Slopes of Linear Trend Lines from Figure 18 (a) 26
Figure 20. Extrapolator for Energy Absorption Process 27
Figure 21. Ground Cavity Data and Predictions 29

Table

.Table 1. Coefficients of Trend Lines in Figure 18(a) 26
Table 2. Data on Ground Crater Diameter Reduction by Intervening RPF Layers 28

Background

During the last few years we have conducted a series of investigations on the military applications of rigid polyurethane foam (RPF) materials. As a part of those investigations we considered the impact of explosive blast waves, fragments and projectiles on the RPF materials of different density. RPF material properties are dependent principally on the material density. Therefore, varying this parameter is most important in studying material responses. In the aforementioned study we determined that the RPF resistance to fragment and projectile penetration was very slight, but that the effect on an incipient blast wave was significant. This was not the first study of these effects. Cooper and Kurowski explored the blast absorbing capabilities of RPF of various densities during the middle 1970s. They considered the cavities produced by charges detonated in the interior of blocks of RPF. By varying the RPF densities and charge weights of explosive (Tetryl) they developed an empirical scaling law.

We extended that work in 1995 and 1996,[1] repeating some imbedded explosions and adding free surface ones as well. The interesting reported result was that the cavity diameter produced by detonation of a given weight of explosive was the same whether the explosive was embedded in the center of the block or lying on the top horizontal (free) surface. Our Phase II report[2] further generalized the conditions to include detonations at the undersurface of a block. We supported the blocks on earth and floated them on water. It also includes one underwater[2] experiment in which the explosive was not in contact with the block. This was done to investigate the possibility of using this material as a protection for ship hulls subjected to nearby explosions, such as from influence mines. We have done no work, to date, on non-contact explosions in air. We believe that this report provides the first published quantitative data on RPF blast energy absorption, based on a series of flyer plate experiments reported therein.

General Plastics Corporation (GP) recently conducted several demonstrations of a commercial product that was empirically designed to attenuate air blast. One of these demonstrations was conducted during the first week in May 1999 at Quantico, Virginia. That demonstration was not planned for data acquisition. However, some information has been extracted from it.

Reduction of the data from these experiments has shown that RPFs have a remarkable and surprising capability to absorb and perhaps to dissipate the energy of a blast wave. Some fundamental questions arise when carefully examining the available data, and when observing explosive events, such as those at Quantico. The actual energy absorbing mechanisms seem quite complex. The possibilities seem to include compression of the gas in the cells, multiple "micro reflections" from the many cells encountered by the blast wave, chemical reactions induced in the gas and in the polyurethane, radiant heat transfer, strain energy in the polyurethane, secondary burning of the affected material, and acceleration of the affected materials. The research required to assess the relative

effectiveness of these, and possibly other mechanisms as well, has not been done. Therefore, at this time the best use of the existing data seems to be in establishing empirical rules for protection of structures.

There seems to be, in spite of the lack of fundamental understanding of mechanisms, a potential to use this material as a protective measure in a number of situations. The possibility of ship hull protection has been mentioned. Another possibility is the protection of concrete structures from a terrorist attack, such as a satchel charge placed in contact, or a larger charge placed some distance away.

An explosive device placed in contact with the structure, and one placed at a distance from it will produce somewhat different effects. We have data sufficient to provide a reasonable estimate of the contact event, though it would be wise to verify the extrapolations described herein with a small number of confirmatory experiments.

Introduction

The purpose of this report is to document the recent work done to quantify the blast energy absorbing capability of the RPF material as well as possible from the existing data, and to suggest appropriate avenues for research to gain better definition of the mechanisms involved. In addition, some potential applications will be suggested. All of the data presented herein are digested from the earlier mentioned reports. This report only considers analysis of those data. Details of the experiments and techniques that produced the data are in those reports.

The basic problem may be posed in two parts: Can RPF material be applied in a useful protective role to prevent damage to structures from explosive devices? If so, how can it be effectively used and what are its limitations? The calculations presented in this report may be most readily applied to the case of contact devices, such as satchel charges, placed against the structure in question. Suggestions for follow-on work to apply to non-contacting charges are presented in brief.

Available Data

The first step is to use all available data to generate some empirical rules relating the blast energy absorbed to the density and thickness of the RPF and the weight of the charge. Those rules will then permit estimation of the effect of the blast wave on the structure behind the RPF layer.

There are four groups of reported applicable data. All are in the aforementioned documents. Three data sets relate the size of the cavity produced in the RPF to the RPF density and charge mass. The first of these reports work by Cooper & Kurowski; the other two, work by Woodfin. These data are presented in aggregate in Figure 1. In this figure the data have been presented in a form

normalized by mass. The five data points with filled symbols, forming a separate group below the rest, are from the third set of data. They were produced by a plate charge in a dimensionally constrained configuration. Clearly, the RPF absorbs energy more efficiently in this geometry, which corresponds closely to a satchel charge placed against a surface. All the other data were produced by essentially spherical charges.

There is one set of "soft" data that were obtained through a serendipitous opportunity. These were obtained during the previously mentioned *Force Protection Equipment Demonstration* event at Quantico, Virginia, May 3 – 7, 1999.

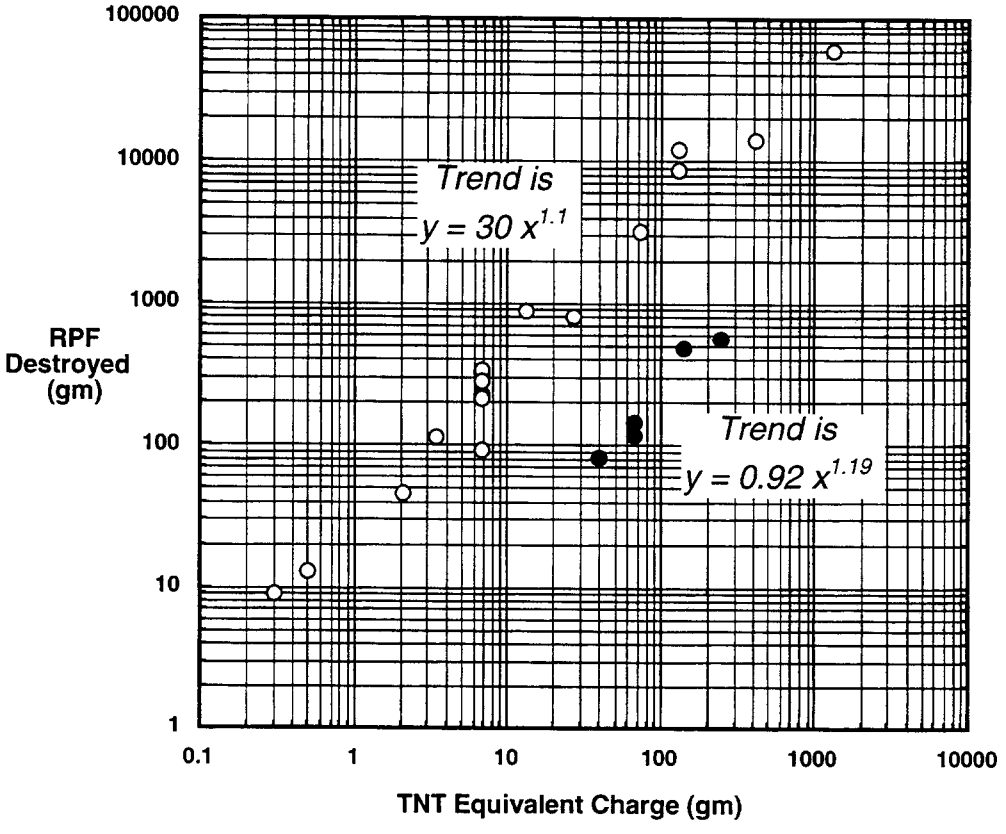

Figure 1. RPF Destroyed in a Variety of Experiments

At this event a large number of vendors of protective products, in addition to GP, exhibited them using explosive charges of different sizes and orientations. In the process a number of ground craters were produced by the different company demonstrations. Those produced in the course of the GP demonstration had RPF intervening between the explosive and the ground; the others did not. Measurement of the crater diameters yielded this set of data. These cannot be regarded as hard data, but interpreting the results in the context of the other data has provided some additional insight. These insights are discussed in a later section of this report.

Cooper and Kurowski used Tetryl to produce the data shown in Figure 2. All these data were produced with totally embedded, nominally spherical charges. They used these data to develop an empirical scaling rule for both charge weight and density:

$$D = \frac{\sqrt[3]{W}}{6.3 + 0.5\rho} \tag{1}$$

where

D is the cavity diameter in meters,
W is the charge mass in grams, and
ρ is the RPF density in pounds per cubic foot (pcf).

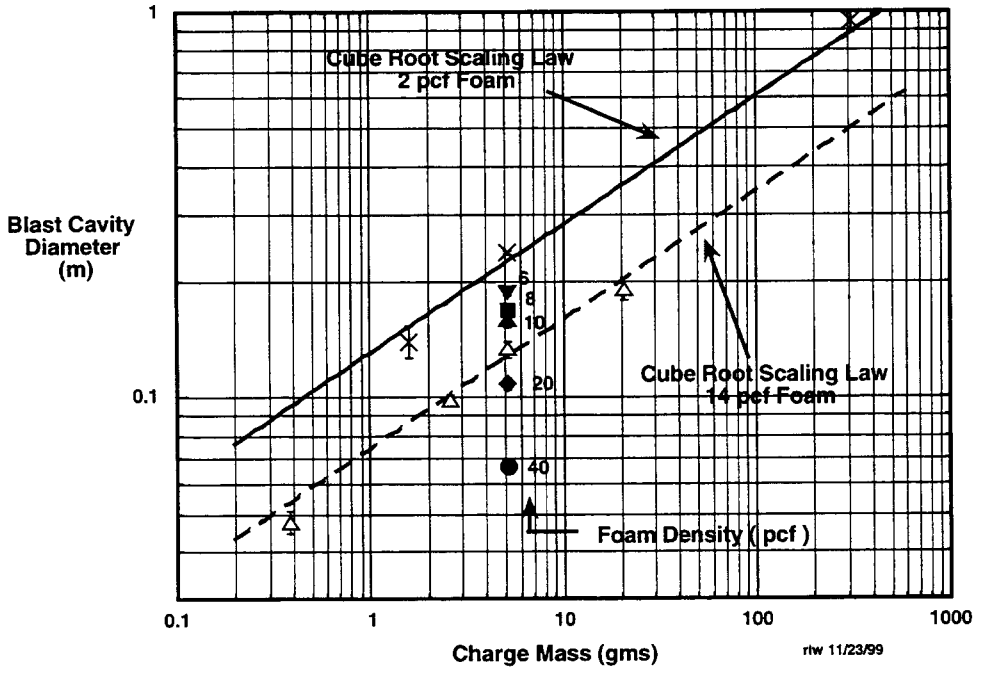

Figure 2. Data from Explosive Tests on Foams (replotted from Cooper & Kurowski, October 6, 1975)

The work that resulted in the second data set established that the cavity size produced was essentially independent of the location of the explosive. That is, a charge of a given mass produced a cavity of the same diameter whether it was imbedded in, on the upper surface of, or under a block of RPF of a particular density. The embedded charges produced nearly spherical cavities, while the surface charges produced hemispherical cavities of corresponding diameter.

Figure 3 illustrates this effect. In this Figure the filled symbols indicate embedded charges; the larger ones represent the data added and the small ones, the original Cooper & Kurowski data set. The "cube root scaling" lines follow those shown in Figure 2, and are calculated using the empirical scaling rule of equation 1, above. In Figures 3 all surface charges were on the upper surface.

This third set, henceforth called the "plane wave cavity data set", differs from a fourth set, called the "flyer plate data set", although both were formed by

firing a charge configured to produce a plane wave of specific diameter normal to the direction of propagation. The cavities formed in the two differed in that the former shots were fired into a thickness of RPF sufficient to contain the cavity, while the latter were fired into RPF layers of specified thickness, backed by a steel plate. These layers were not sufficient to contain the cavity, since the objective was to accelerate the flyer plate.

This flyer plate data set proved to be the most useful for the purposes of this study. It was developed by firing plane wave charges[2] through a sheet of RPF to accelerate a steel flyer plate. The apparatus is shown diagrammatically

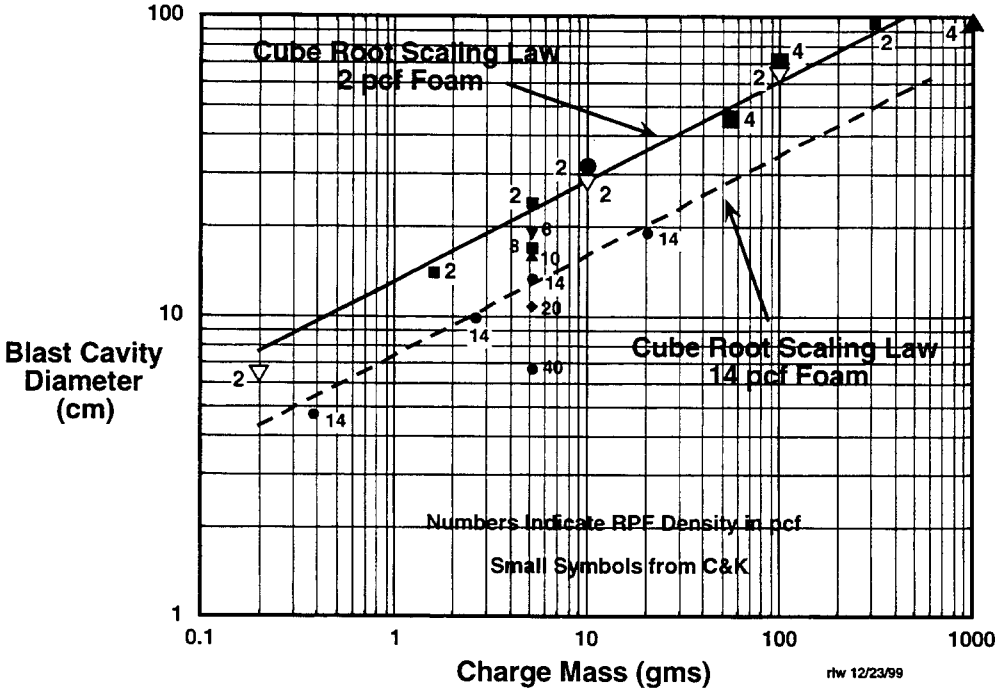

Figure 3. Data from fully Embedded Explosive Tests on Foams (replotted from Cooper & Kurowski, October 6, 1975) {Embedded & Surface Charge Data Added by Woodfin @EMRTC Nov & Dec, 1996}

in Figure 4. The velocity of the flyer plate was used to calculate the energy absorbed by the RPF sheet. This energy absorbed became the basis for the following calculations. Flyer plate velocity data was gathered only for 5.7 pounds per cubic foot (pcf) RPF; plane wave cavity data was collected for 3.3 pcf and 5.7 pcf RPF.

The first data[3] was collected using Tetryl; the rest,[1,2] using C-4 and PETN. Consequently, the data is normalized to TNT equivalence in the following sections. This is appropriate since TNT is the standard for comparison and is also one of the most common explosives found in terrorist devices, because it is readily available and cheap. Figure 5 graphs Equation 1 for both Tetryl and TNT, illustrating the minor difference in performance between the two explosives.

Analysis of Cavity Formation Data

The effect of density is seen to be modest, especially for densities of less than 10 pcf. The similarity in the results for the plane wave and spherical charge cavity experiments seen in an examination of Figure 1 suggests that assuming a similar relationship to hold for the former should be justified.

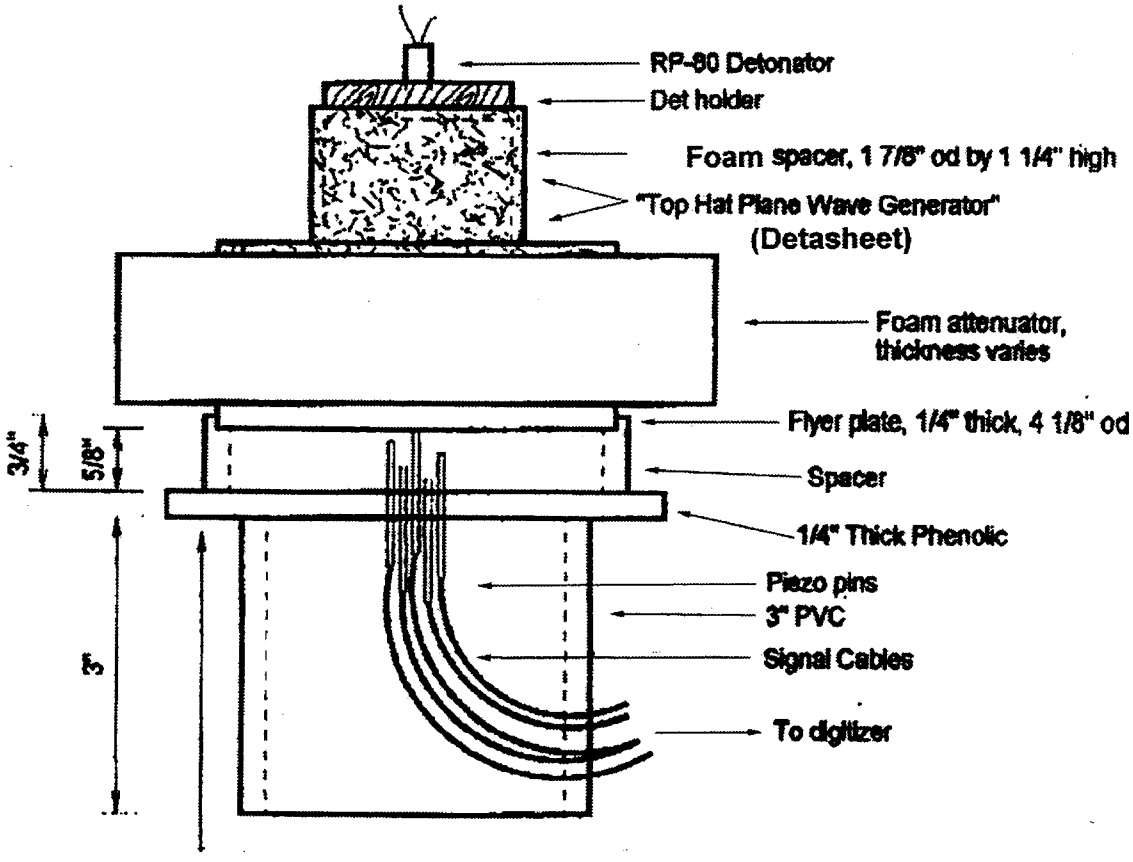

Figure 4. Diagram of Flyer Plate Apparatus
(See Reference 2 for More Details)

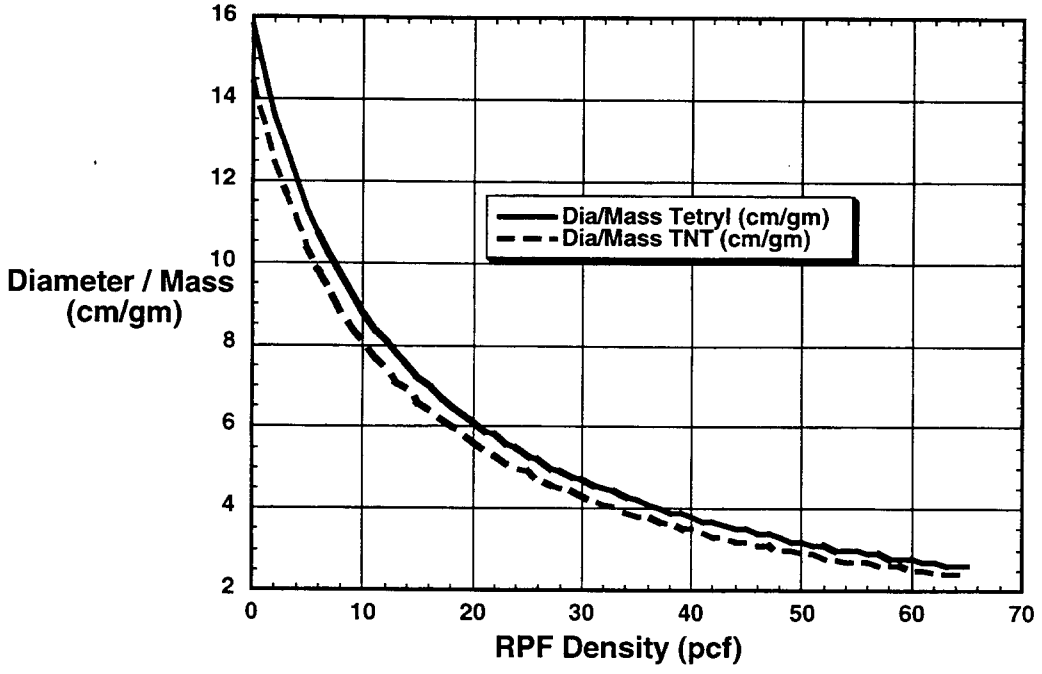

Figure 5. Cavity Diameters Produced in RPF by Tetryl and TNT Unit Charges (from Cooper & Kurowski Formula)

In fact, by recasting the relationship in terms of volume, V, of RPF destroyed in a spherical, imbedded shot such as Cooper and Kurowski used, the relation takes the form:

$$V = \frac{4\pi W}{3(12.6+\rho)^3} \tag{2}$$

where

V is the volume of the hypothetical spherical cavity in the RPF, in m^3,
W is the mass of explosive in grams, and
ρ is the RPF density in pcf.

(The hybrid system of units adopted by Cooper and Kurowski is continued here. This conforms to the normal industry practice of describing RPFs in terms of their density in pcf. It is thus implied that the empirical value 6.3 in equation 1 is a density quantity, to be expressed in pcf.)

In equation 2 the volume depends linearly on the charge. Therefore, using the assumption that the cavity produced is spherical, it is possible to calculate the mass of RPF destroyed in the cavity volume by a unit mass of explosive. The mass of the RPF is merely the product of the density and volume, so that the "mass destruction ratio" becomes:

$$\frac{W_{RPF}}{W_{Expl}} = \frac{12.87\rho V}{W_{Expl}} = \frac{53.89\rho}{(12.6+\rho)^3} \tag{3}$$

where

W_{RPF} is the mass of the RPF destroyed, in grams

12.87 is the factor required to reconcile the units, in gm-ft^3/lb-m^3, and

W_{Expl} is the mass of the explosive used, in grams.

It is easily shown that this equation has a maximum value at an RPF density of 6.3 pcf. Even though the experiments from which this function was established used only Tetryl as the explosive, there, this maximum is assumed to be effectively independent of the explosive used. Figure 6 illustrates the function for Tetryl and scaled for TNT. The existence of a maximum is to be expected, even though we do not understand all the energy absorbing mechanisms. Since it is observed that polyurethane in a rigid foam form absorbs energy more effectively than in the form of solid polyurethane, it is to be expected that some density is the most effective. It has not been proven that the maximum in the destruction ratio establishes that value. Some other mechanism may dominate, but it presents a starting place for isolating the density for peak efficiency.

If we make the plausible assumption that the shape of the cavity is of secondary effect, then this relation should apply to the roughly cylindrical cavities produced in the plane wave cavity shots. These cavities approach oblate spheroids in shape. Figure 1 does give reason to question this assumption, but for purposes of estimating the thickness of RPF needed for absorption of a given charge energy the error in this assumption tends toward conservative results.

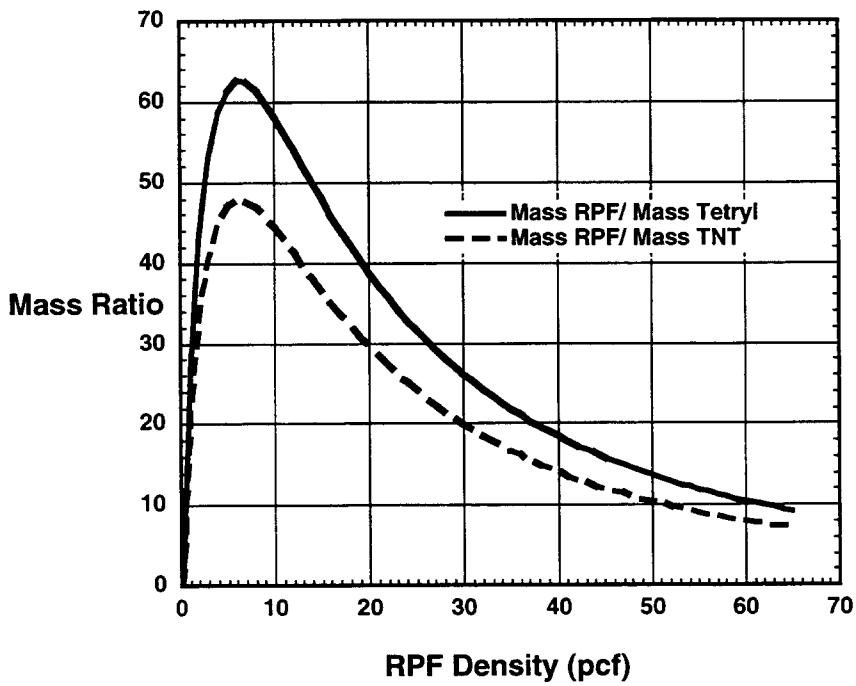

Figure 6. Mass of RPF Destroyed by Tetryl & TNT Unit Charges (from Cooper & Kurowski formula)

Analysis of Flyer Plate Data

The flyer plate experiments used three different size charges of PETN, each arranged so as to develop a plane wave for propelling the plate with its velocity vector normal to its surface. Sheets of RPF of varying thickness were placed between the charges and the steel flyer plates so as to absorb energy from the explosive prior to accelerating the plate. The plate velocities were then measured. Figure 7 presents this data. The physical form of the experiments has been described in detail.[2]

Obviously, the explosive energy is absorbed effectively by these RPF sheets. The geometry of this experiment causes the blast energy to be absorbed principally in the cylinder of RPF between the explosive and the flyer plate. It appears that the presence of the flyer plate may be the major contributor to the greater energy absorption effectiveness observed in Figure 1. The effect of the plate (or a supporting structure behind the RPF) seems to be in delaying the motion of the RPF by its greater density. This, perhaps, allows some of the other hypothesized mechanisms to develop more fully.

Therefore, using the diameter of the flyer plate and the thickness of the RPF sheet being used as the attenuator, it becomes possible to directly determine the volume and mass of RPF destroyed in attenuating the blast wave. From this and

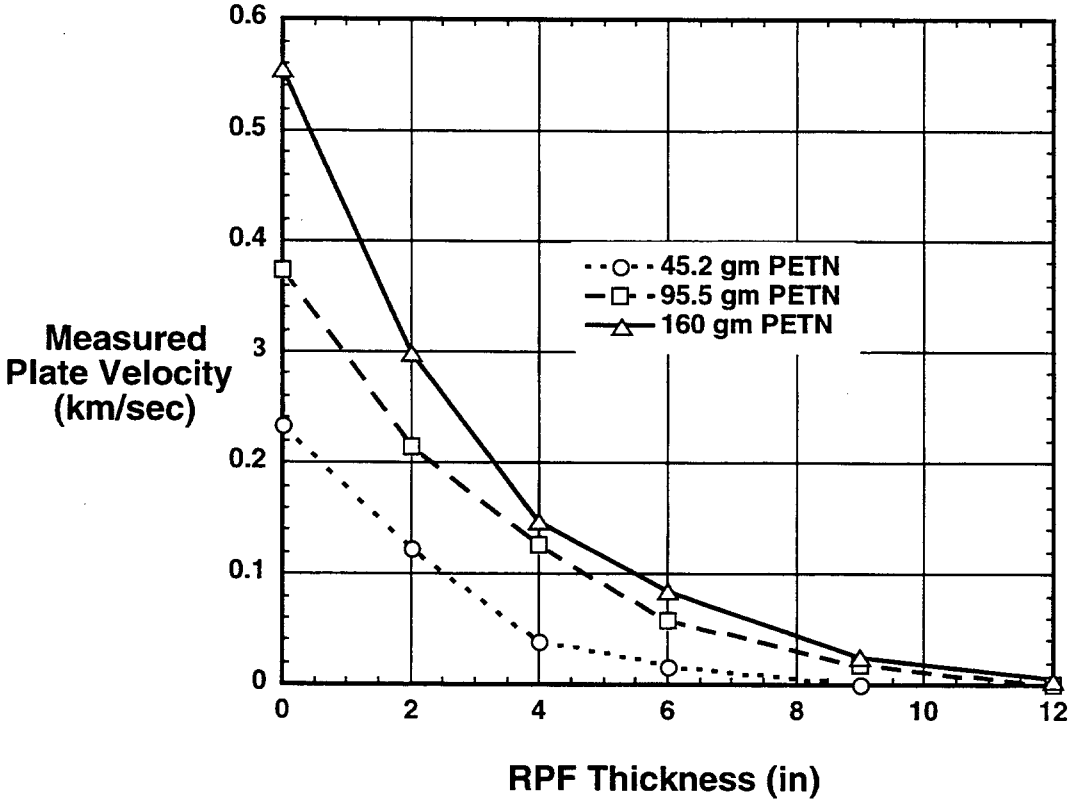

Figure 7. Flyer Plate Velocity Attenuation by 5.7 pcf (RPF

the reduction in kinetic energy it is possible to calculate the absorption energy density, *i.e.*, the energy absorbed per unit volume of RPF, of the process through each incremental layer of the attenuator. The equation is

$$\overline{E} = \frac{KE_a}{V_{RPF}} = \frac{m\left(u_i^2 - u_f^2\right)}{2V_{RPF}} \tag{4}$$

where

$\overline{E}$ is the absorbed energy density, the bar denoting the energy density,
KE_a is the attenuated kinetic energy of the flyer plate,
V_{RPF} is the volume of RPF absorbing energy,
m is the mass of the plate,
u_i is the initial velocity of the plate, and
u_f is the final velocity of the plate.

Figure 8 displays the absorption energy density as measured in the flyer plate experiments. This quantity is directly related to the "Mass of RPF Destroyed" in Figure 1. This figure illustrates the development of the energy absorption as the blast wave propagates through the RPF.

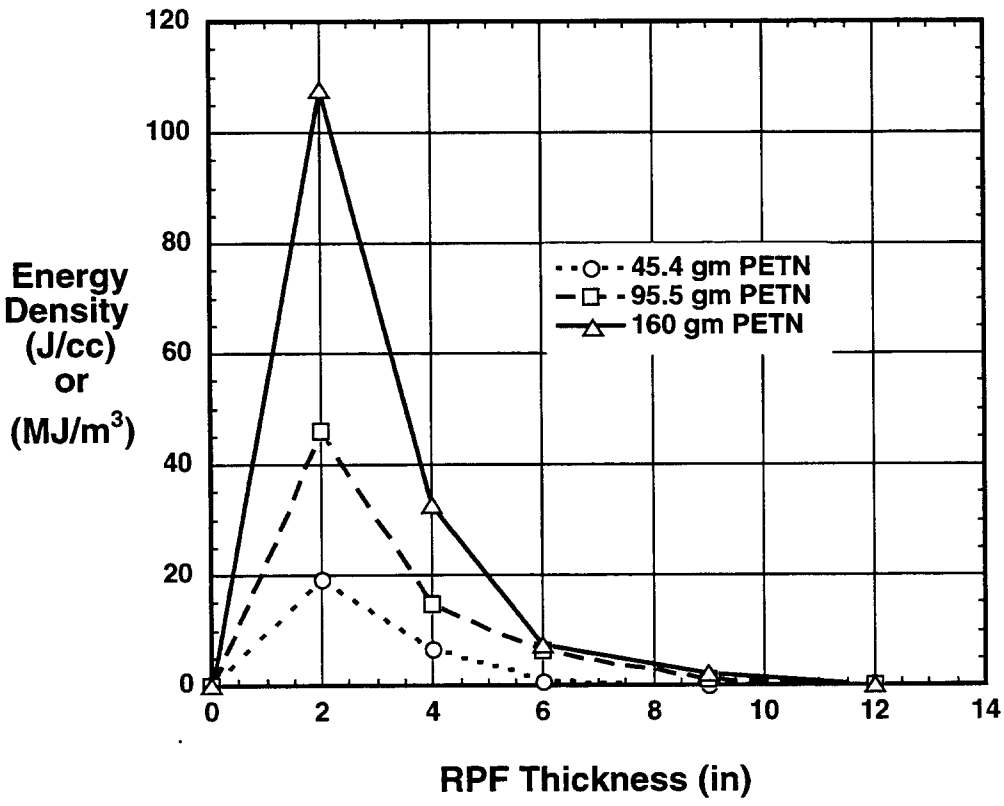

Figure 8. Incremental Energy Density Absorbed in 5.7 pcf RPF layers

The cumulative effect is obtained by the summing the energy density absorbed over the total thickness of RPF used. The mathematical process is

$$\overline{E} = \sum_{n=1}^{N} \overline{E_n} \tag{5}$$

where

n denotes the nth layer of the RPF attenuator and

N is the total number of layers.

Figure 9 illustrates the cumulative effect of several inches of RPF. The two figures (8 and 9) show that the layers that encounter the blast wave first do the greatest rate of attenuation. The energy remaining for the deeper layers to attenuate is substantially less, on a volumetric basis. This tempts one to speculate that the mechanisms of attenuation accomplish much of their work by internal reflections and refractions at cell boundaries to weaken the wave structure. Research is needed to determine these mechanisms.

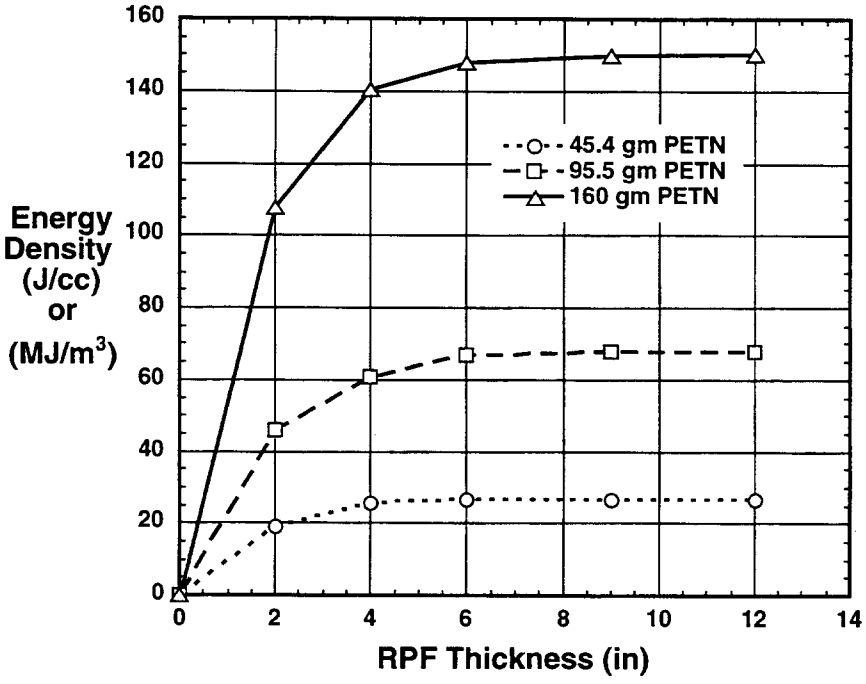

Figure 9. Cumulative Energy Density in 5.7 pcf RPF from PETN Plate Charge

Two other related quantities are useful to calculate, the total energy absorbed, E, and the total specific energy absorbed, $\hat{E}$. The first is found by any of several calculations:

$$E = \sum_{n=1}^{N} E_n = \sum_{n=1}^{N} KE_{a_n} = \frac{m}{2} \sum_{n=1}^{N} \left(u_{i_n}^2 - u_{f_n}^2 \right) = \sum_{n=1}^{N} \overline{E_n} V_n \tag{6}$$

where

E_n is the energy absorbed in the nth layer, (with small error the total energy absorbed can be considered to be only the kinetic energy attenuated)

KE_{a_n}

is the kinetic energy attenuated in the nth layer

m is the mass of the flyer plate,

V_n is the volume of RPF destroyed in the nth layer of the attenuator,

u_{i_n} is the *constructive* initial velocity of the plate for layer n, considering it to have been produced by a charge attenuated by layers $1,\ldots, n-1$,

u_{f_n} is the *constructive* final velocity of the plate for layer n, considering it to have been produced by a charge attenuated by layers $1,\ldots, n$.

In each case

$$u_{i_{n+1}} = u_{f_n} \tag{6a}$$

This variation in total energy is illustrated in Figure 10, with the RPF thickness in centimeters to facilitate further analysis.

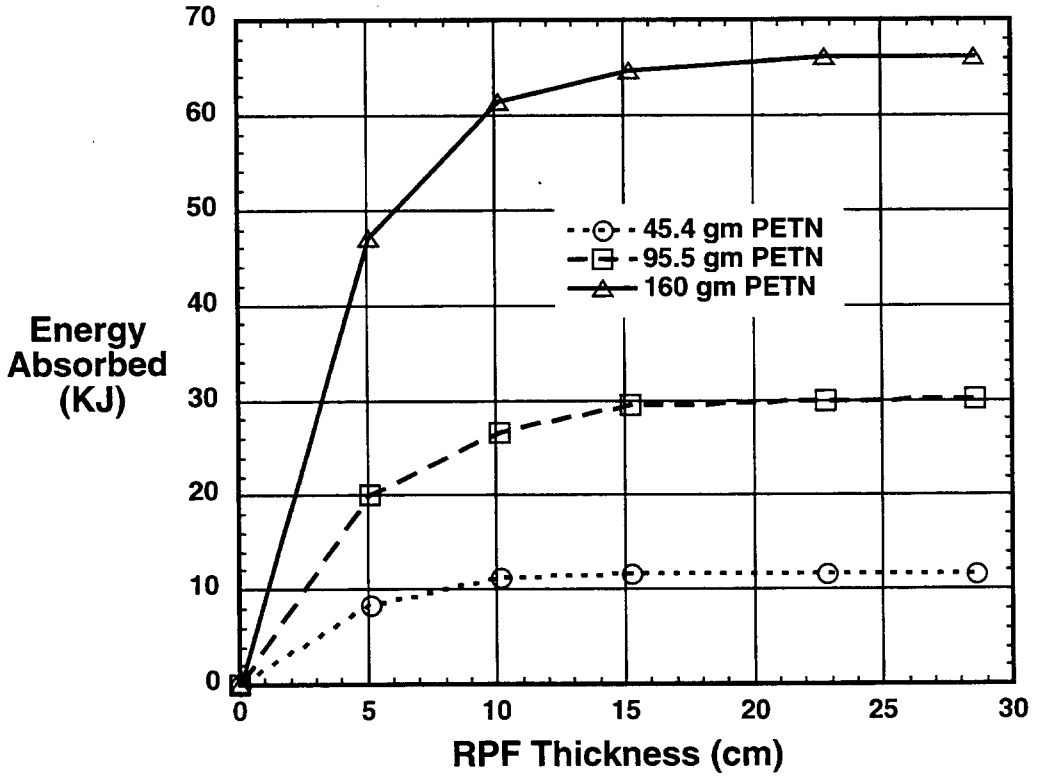

Figure 10. Total Energy Absorbed by 5.7 pcf RPF

The other useful quantity is the normalization of the energy absorbed on the basis of the explosive mass, that is, the specific absorption energy is that which is absorbed by a unit mass of explosive, in this case PETN. This normalization will lead to a form of the process description that will permit extrapolation to larger explosive charges. It is characterized by

$$\hat{E} = \sum_{n=1}^{N} \hat{E}_n = \sum_{n=1}^{N} \frac{E_n}{W_{Expl}} = \frac{1}{W_{Expl}} \sum_{n=1}^{N} E_n \tag{7}$$

where

^ (caret) superposed signifies the specific energy. Figure 11 then presents the total specific energy absorbed.

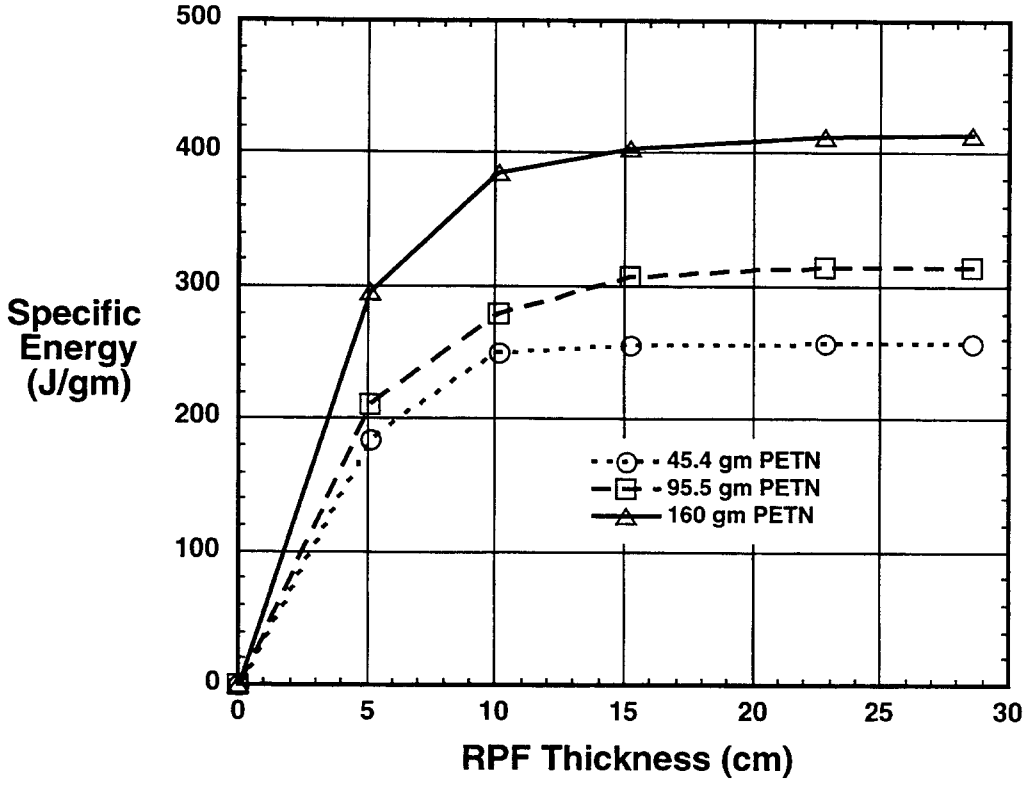

Figure 11. Total Specific Energy Absorbed by 5.7 pcf RPF

The two normalizations may be combined to form the absorbed specific energy density by dividing the specific energy absorbed by the volume of RPF destroyed in each layer:

$$\bar{\hat{E}} = \sum_{n=1}^{N} \frac{\hat{E}_n}{V_n} = \frac{1}{W_{Expl}} \sum_{n=1}^{N} \bar{E}_n = \frac{1}{W_{Expl}} \sum_{n=1}^{N} E_n \tag{8}$$

as shown in Figure 12.

No matter which data presentation is used, it becomes readily apparent that the majority of the available energy is absorbed in the first four inches (ten centimeters) of the RPF, with almost all being absorbed by the first nine inches. In fact, very little is energy remains after six inches are destroyed. This is consistent with the underwater[2] standoff shots as well, where 1.5 inches of 3.3 pcf RPF were sufficient to prevent major structural damage in the experimental

panels. An earlier attempt at suppressing underwater shock damage using rigid epoxy foams was unsuccessful.

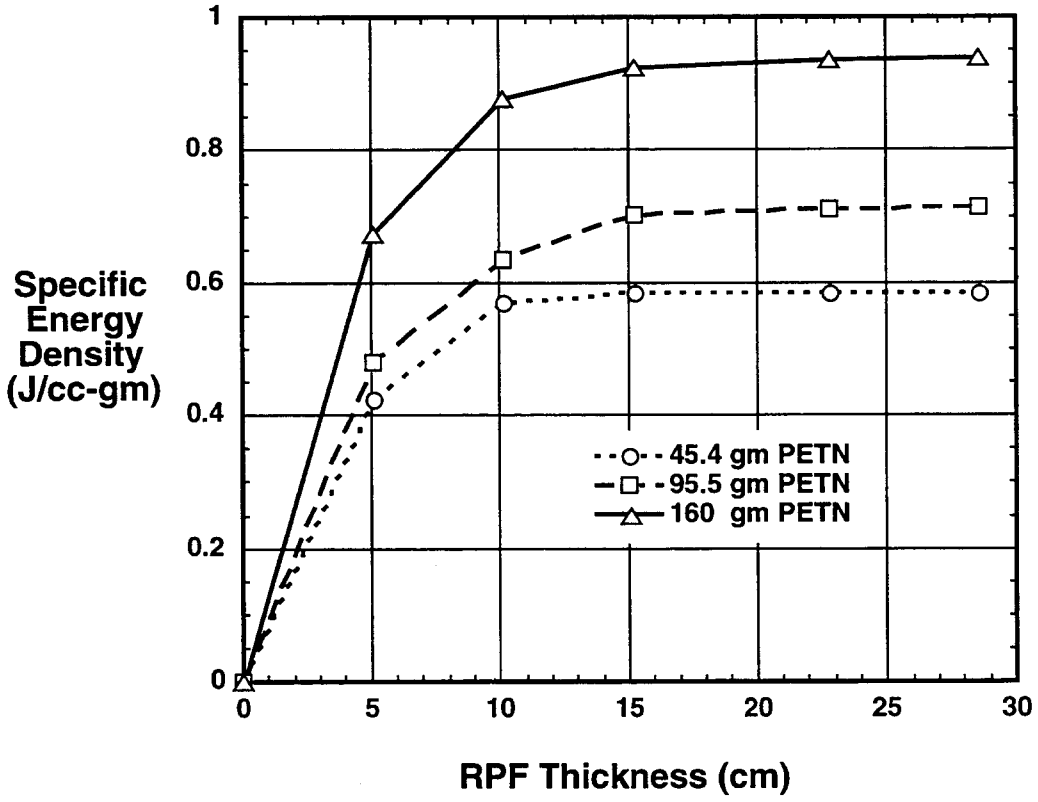

Figure 12. Total Absorbed Specific Energy Density of 5.7 pcf RPF

Adjustment for Density and Explosive Used:

This absorbed specific energy density forms a most useful measure of the energy absorbing capability of the RPF of the density under consideration. It is necessary to adjust it to the density of interest. While the Cooper-Kurowski equation suggests a way to do this, it requires a rather weakly substantiated assumption, to wit, that that the volume of RFP destroyed in the cylindrical geometry of the flyer plate experiments is represented by the volume term in the spherical geometry of the cavity experiments. The quality of this assumption has not been established. One procedure for adjusting for the RPF density would be to consider the ratio of volumes consumed by equal explosive charges in RPFs of different density. Using equation 2 that ratio takes the form

$$\frac{V_1}{V_0} = \frac{(12.6+\rho_0)^3}{(12.6+\rho_1)^3} \tag{9}$$

where the subscripts simply indicate two different RPF densities. For a given value of the baseline density this ratio varies monotonically. This result defies intuition, since neither air nor solid polyurethane is expected to be as effective as some intermediate density, based on the cavity experiments. An optimum is to be expected. If Figure 6 is an accurate guide, then the optimum density for most applications will be near 6.3 pcf. By using a mass ratio instead of a volume ratio, a maximum is achieved at that point, following the relation:

$$\frac{W_1}{W_0} = \frac{\rho_1 (12.6 + \rho_0)^3}{\rho_0 (12.6 + \rho_1)^3} \tag{9a}$$

which does exhibit a maximum at $\rho_1 = 6.3$ pcf, for any value of ρ_0. That may be misleading, however. Additional experiments are necessary to understand this process more thoroughly.

The specific energy density form also permits adjustment to the explosive of interest. It is most useful to use TNT as a baseline. PETN has 1.45 the energy of TNT; Tetryl, 1.31 times. The advantage of normalizing by the charge will be seen later. Figure 13 illustrates the energy density. Figure 14 employs the specific energy density. In these figures the independent variable has been changed to be the TNT equivalent charge. Clearly a linear model is a better approximation of the process when using the specific energy density.

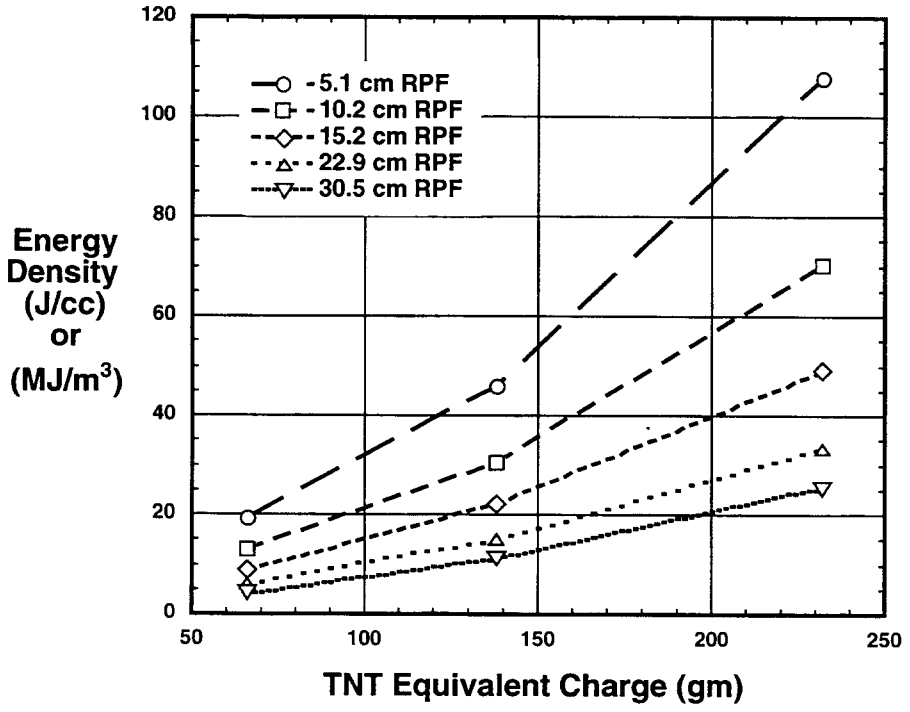

Figure 13. Absorbed Energy Density in 5.7 pcf RPF from PETN Plate Charges

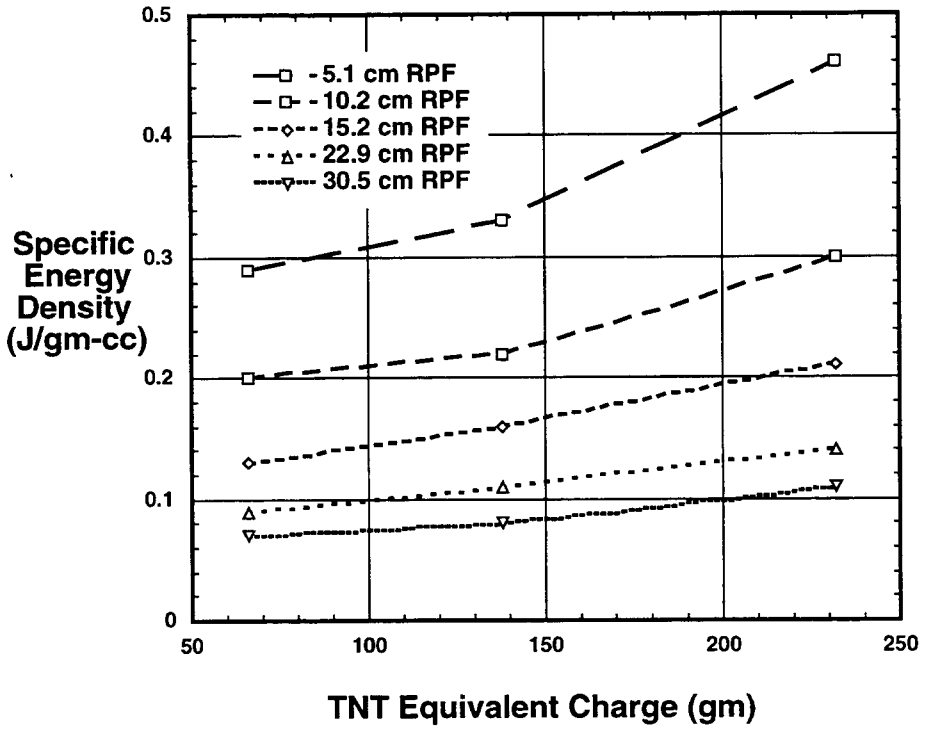

Figure 14. Specific Energy Density Absorbed from PETN Plate Charges in 5.7 pcf RPF

Extrapolation to Larger Explosive Charges

Using the absorbed specific energy density it is possible to then calculate an even more useful quantity that relates the energy absorbed to the area of the surface impinged by the wave. This is particularly true since the proposed application to anti-terrorist protection systems will always be directed toward a surface or off-surface charge, likely never an embedded one. Because of its relationship to the area, this quantity is appropriately considered as a flux. For the flyer plate experiment this area is well defined by the area of the plane wave, which is the same as that of the flyer plate, 86 cm^2. The flux is obtained by dividing the absorbed energy by the effective area, or equivalently for the flyer plate experiments, by multiplying the absorption density by the thickness of the absorbing RPF. The flux is denoted by the "dish", or "smile" symbol. The incremental absorbed energy flux is:

$$\breve{E}_n = \frac{KE_{a_n}}{A_n} = \overline{E}_n t_n \tag{10}$$

where

A_n is the effective area of the nth RPF layer and

t_n its thickness,

so that

$$V_n = A_n t_n \tag{11}$$

The total absorbed energy flux is computed by

$$\breve{E} = \sum_{n=1}^{N} \breve{E}_n = \sum_{n=1}^{N} \overline{E}_n t_n \tag{12}$$

and shown is in Figure 15. The specific energy flux absorbed is the more useful quantity for extrapolation and application, since it is much better represented by a linear extrapolator, especially as the RPF thickness becomes adequate to absorb most of the energy:

$$\breve{\hat{E}}_n = \frac{\breve{E}_n}{W_{Expl}} \tag{13}$$

Therefore, using equations 7 and 11, the total absorbed specific energy flux is

$$\breve{\hat{E}} = \sum_{n=1}^{N} \breve{\hat{E}}_n = \frac{1}{W_{Expl}} \sum_{n=1}^{N} \overline{E}_n t_n \tag{14}$$

This total absorbed specific energy flux is shown in Figure 16.

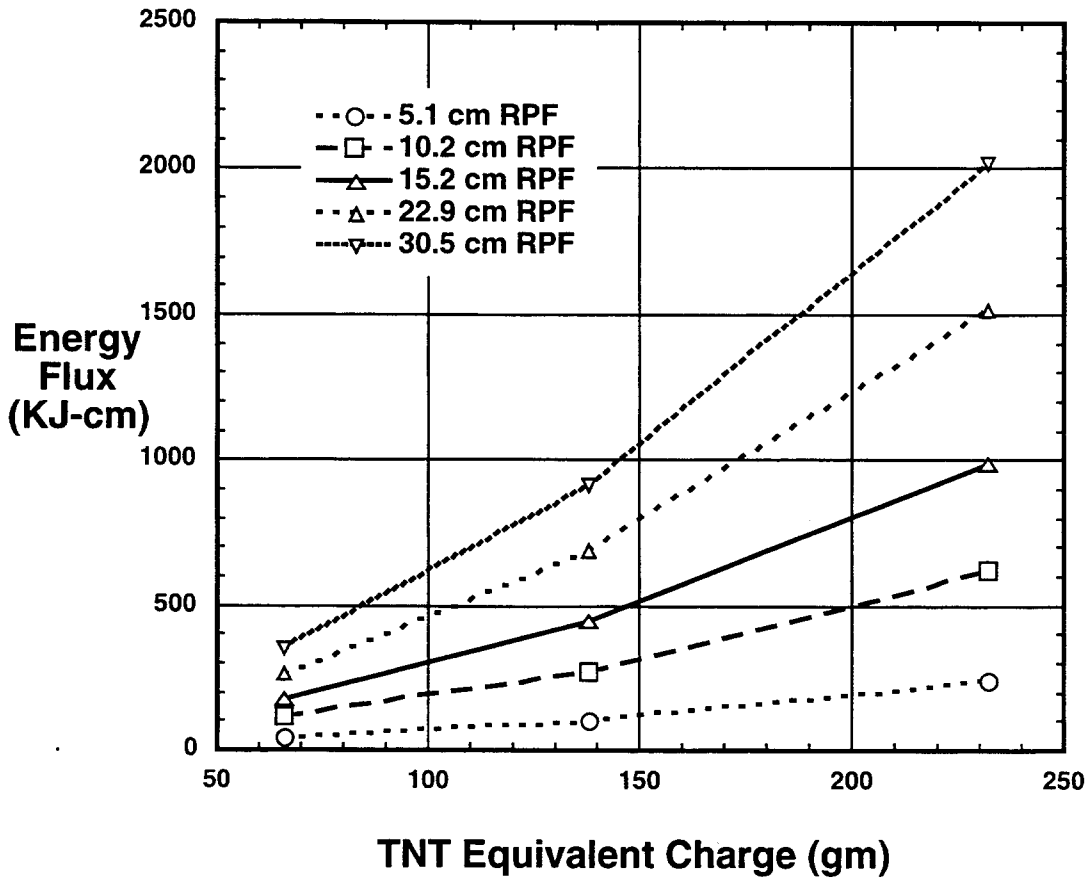

Figure 15. Energy Flux Absorbed by 5.7 pcf RPF from PETN Plate Charges

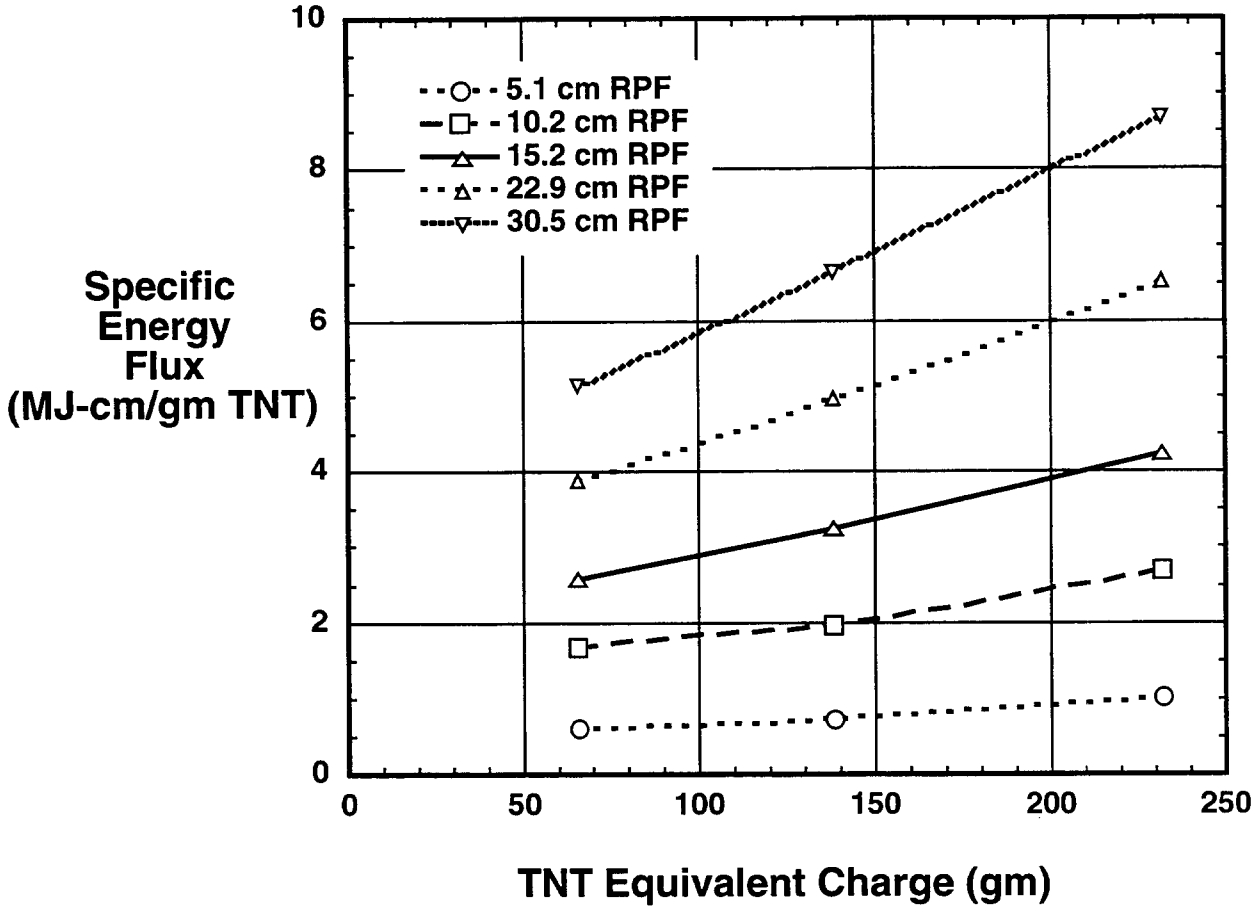

Figure 16. Specific Energy Flux Absorbed in 5.7 pcf RPF by PETN Plate Charges

As in the case of the density, above, the advantage of using the specific form is apparent, as it provides a more nearly linear data description. Combining the density and flux normalizations produces an interesting result. In Figure 17 the RPF thickness is observed to become a less dominant parameter in this description of the process. As noted earlier, the first few inches of the RPF encountered by the blast wave absorbs the energy most rapidly. After the wave traverses about six inches (ten centimeters) of RPF the energy absorption rate becomes more nearly constant. For predictive purposes, especially when more than six inches of RPF are used, the effect of thickness may be regarded as a secondary parameter.

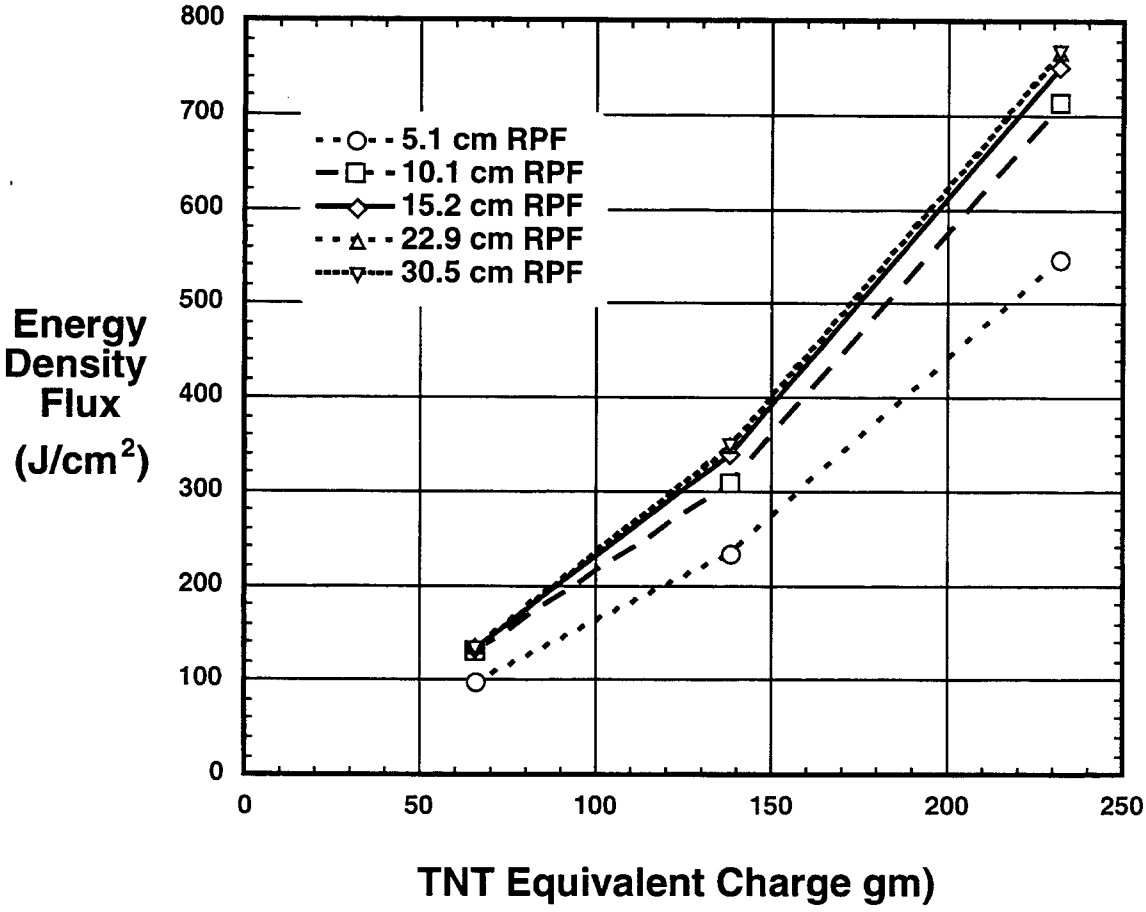

Figure 17. Energy Density Flux Absorbed in 5.7 pcf RPF from PETN Plate Charge

This effect is maintained when all the normalizations, including the specific form, are used simultaneously, as in Figure 18. This combination provides the most effective predictor form.

In of Figure 18 a trend line has been calculated for each set of data plotted. These are shown in Figure 18(a), where the line connecting the data points in Figure 18 has been replaced by the trend line for each set of data points. The error bars shown indicate a five percent data scatter, or uncertainty. Examination of Figure 18(a) shows that the quality of the predictive ability of the trend lines improves rapidly as the RPF thickness approaches the 30 cm value. In fact the small differences in the trend line equations for the 15.2, 22.9 and 30.5 cm thicknesses are within the scatter of the data. Therefore, it is proposed that a simplified extrapolator may be realistic.

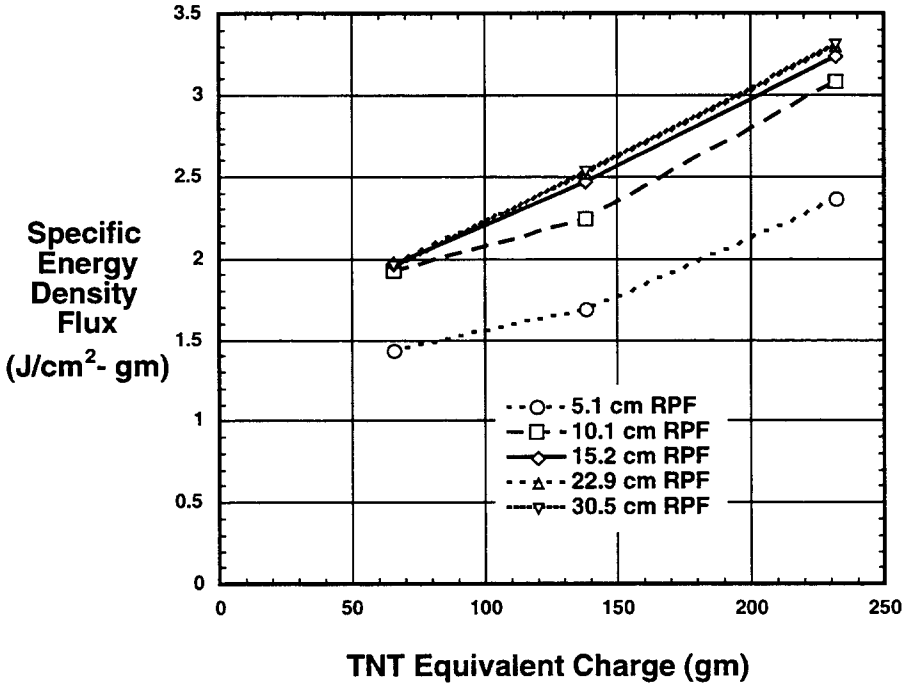

Figure 18. Specific Energy Density Flux Absorbed in 5.7 pcf RPF from PETN Plate Charges

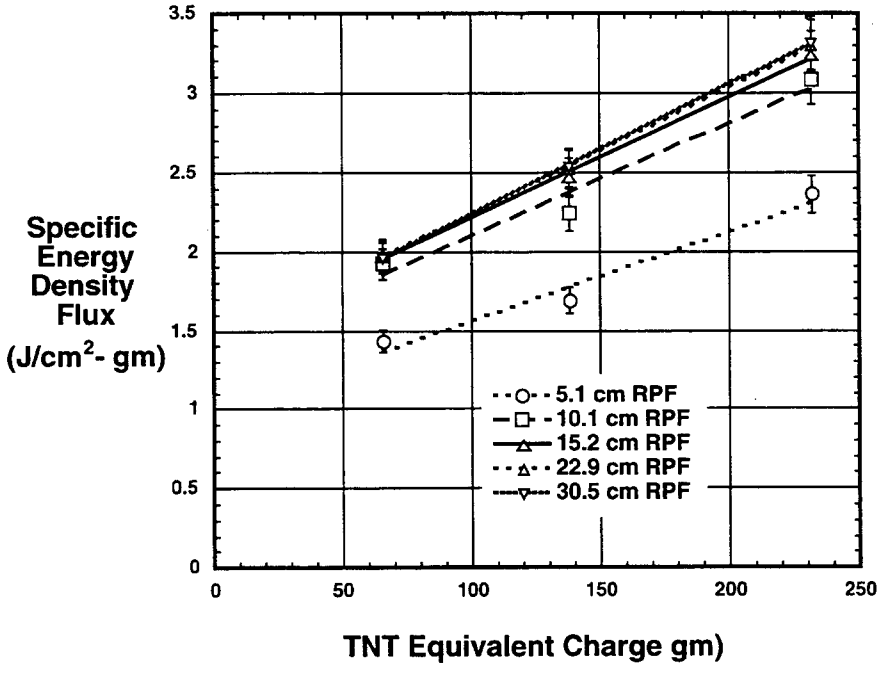

Figure 18(a)

Trend Lines of Specific Energy Density Flux Absorbed in 5.7 pcf RPF form PETN Plate Charges

Figure 18(a) Trend Lines of Specific Energy Density Flux Absorbed in 5.7 pcf RPF from PETN Plate Charges

The trend lines of Figure 18(a) are seen to converge for the greater thicknesses of the RPF. The trend lines all take the form

$$\tilde{\tilde{E}} = A + QW_{TNT} \tag{15}$$

where

Q is the slope of the trend line in J/(cm-gm)^2

A is the ordinate axis intercept (with little apparent significance), and

W_{TNT} is the TNT equivalent charge in grams.

As the trend lines converge their slopes seem to approach a limit. This limit, from observation of the effect in Figure 19, is about 0.0083 J/(cm-gm)^2. Table 1 lists the coefficients of the trend lines in terms of Equation 15. The slopes from Table 1 are shown in Figure 19.

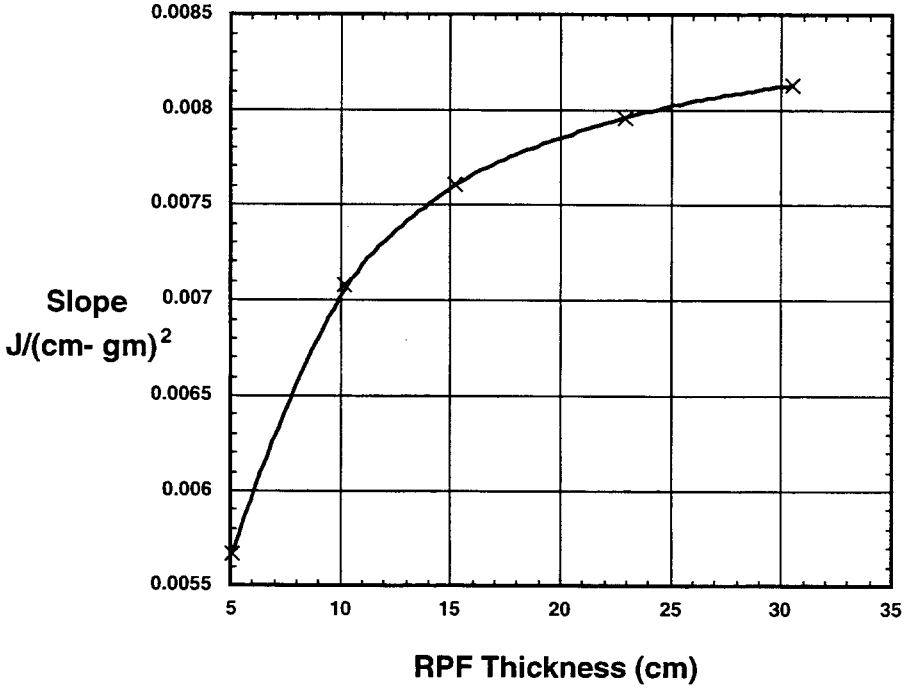

Figure 19. Slopes of Linear Trend Lines from Figure 18 (a)

Table 1. Coefficients of Trend Lines in Figure 18(a)

RPF Thickness (cm)	Axis Intercept (A) [J/(cm^2-gm)]	Slope (Q) [J/(cm-gm)^2]	Goodness of Fit Ratio
5.1	1.0029	0.0056710	0.98496
10.2	1.3855	0.0070758	0.98426
15.2	1.4518	0.0076060	0.99908
22.9	1.4437	0.0079597	0.99958
30.5	1.4188	0.0081314	0.99990

With the foregoing established, it is possible to form an extrapolator for this data. Figure 20 is formed by plotting the data shown on Figures 18 and 18(a), with the addition of a simple extrapolator of the form

$$\breve{\breve{E}} = 1.4 + 8.3 W'_{TNT} \tag{16}$$

where

W'_{TNT} is the TNT equivalent charge expressed in *kilograms*, as signified by the prime. The parameters are estimated from the trends observed in Figure 19 and Table 1.

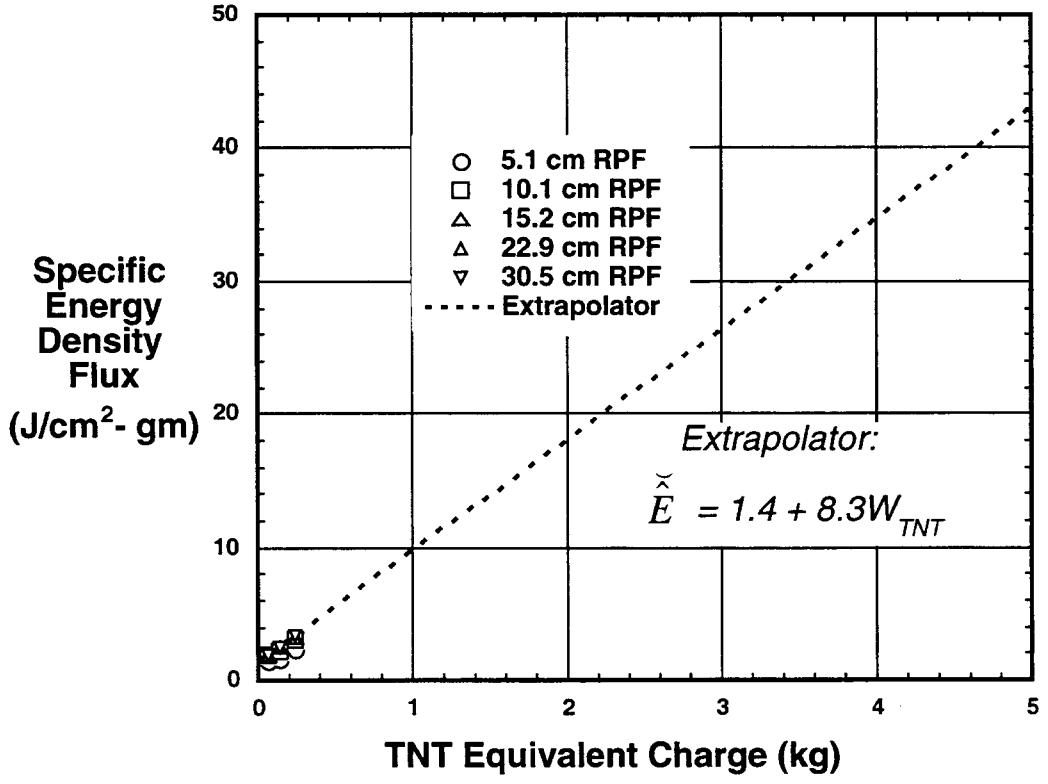

Figure 20. Extrapolator for Energy Absorption Process

Experience with these materials and explosives indicates that the process should be well described by this extrapolation. However, such extrapolations often hold surprises. Therefore it is obvious that confirming experiments are needed. Some have been proposed, but are not funded as of this writing.

Investigation of Reduction in Ground Crater Size by RPF Layer

Some corroborating information about the ability of the RPF material to be useful in this manner may be gained from the impromptu experiment conducted at Quantico. Since there were many demonstrations being conducted, it was necessary to use any that would apply. Several of the demonstrations were conducted by firing TNT charges on the ground near a protective system being demonstrated by some hopeful vendor. The USMC EOD personnel conducting the firings had prepared and distributed a program for the demonstrations. This program listed the explosive and quantity for each demonstration. Following all the demonstrations the ground craters produced were measured, and compared with the published size of the corresponding charge in the program. The GP demonstrators assisted by supporting their demonstration charges on sheets of RPF. (This support had no effect on their demonstration, but formed a convenient way of raising the charge to the level they needed.) The craters produced by these charges were measured in the same manner as the non-RPF supported charges. These "data" are tabulated in Table 2 and shown on Figure 21. It is an interesting observation that the linear trend line describes the cavity data better than the cube root scaling line.

Figure 21 also includes some calculations of craters sizes made with the "CONWEPS" code. Calculations were adjusted to represent the Quantico soil by applying an 82% reduction in the prediction for dry sand. That caused the computation to match the mean of the data for one charge size. The predictive quality of the CONWEPS code is not known precisely, but the relative effect of the surface burst and the air burst one foot above ground are likely dependable. Comparison of the two RPF data points with the air-burst calculation indicates that the RPF is substantially more effective than an air separation in reducing cavity size. While this information does not fit directly into the foregoing analysis, it is compatible with the results.

Table 2. Data on Ground Crater Diameter Reduction by Intervening RPF Layers

Charge Weight (lb TNT)	RPF Layer Density (pcf)	RPF Layer Thickness (in)	Ground Crater Diameter (in)
25	0	0	48
25	0	0	36
50	0	0	78
50	0	0	76
50	0	0	88
50	0	0	72
40	4	12	32
40	7	12	21

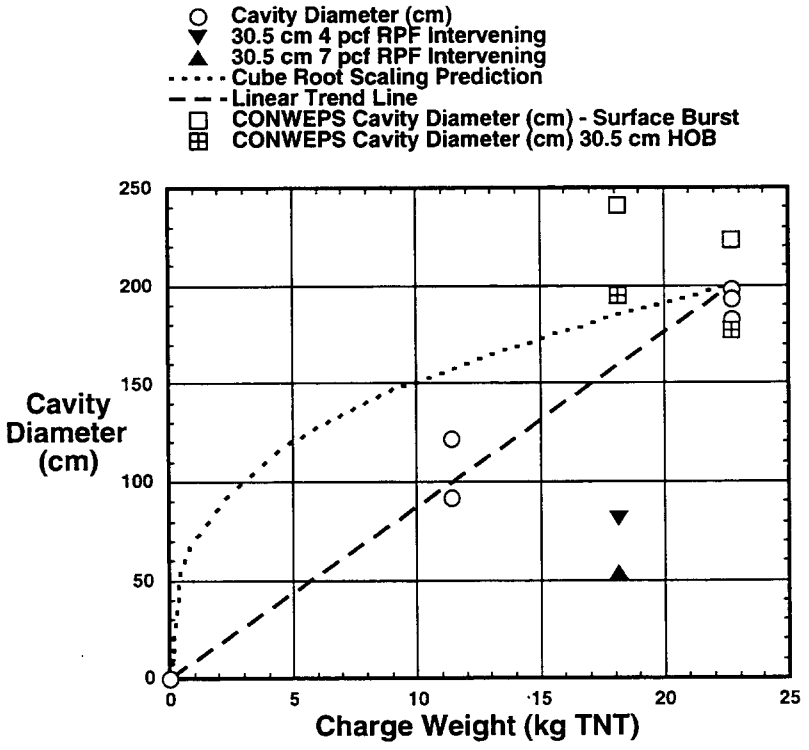

Figure 21. Ground Cavity Data and Predictions

Conclusion

It does appear that RPF can form a valuable tool in protecting structures against blast, such as from terrorist attack. The confirming experiments are necessary to make intelligent design decisions, but, as an interim, a 9 inch thick layer of 6 to 8 pcf RPF can be considered sufficient to greatly reduce damage, especially interior spall from concrete walls in a variety of attack scenarios. As shown earlier, a 6 inch layer is almost as good.

This analysis has considered only blast wave damage. RPF should not be used for protection against explosively driven fragments[2]. Also, this analysis did not consider the effect of the pressure pulse on the overall structure. That is a separate issue. RPF may help some in mitigating that effect, but that is probably not its best use.

References

1. Woodfin, R. L, Rigid Polyurethane Foam (RPF) Technology for Countermines (Sea) Program, Phase I, Sandia Report, SAND 96-2841, January, 1997
2. Woodfin, R. L., D. L. Faucett, B. G. Hance, A. E. Latham, & C. O. Schmidt, Rigid Polyurethane Foam (RPF) Technology for Countermines (Sea) Program, Phase II, Sandia Report, SAND 98-2278, October 1998.
3. Cooper, P. W., & S. R. Kurowski, *Scaling Blast Cavity Diameters in Rigid Foam*, Sandia Laboratories memo of October 6, 1975
4. Giacofci, T. A, & Costanzo, A. A., *An Investigation of Underwater Explosion shock Mitigation Effectiveness of Rigid Syntactic Foam Materials, LATA Report CT00106(01)*, Los Alamos Technical Associates, Inc., Fairfax, VA, for the Defense Advanced Research Projects Agency, Advanced Submarine Technology Program., April 1990.
5. Johnson, D. R. & Fischer, S. H., TNT Equivalence of Energetic Materials, Sandia National Laboratories Explosive Components Facility OP-905-0009, Issue B, Appendix A, p 7
6. Hyde, D. W., CONWEPS Computer code, implementing the equations in US Army TM 5-855-1, USAEVES/SS, 1 May, 1989, Reference:WES Instructional Report SL-88-

Distribution

1 U.S. Department of Energy
Albuquerque Operations Office
Post Office Box 5400
Albuquerque, NM 87185-5400
Attn: Daniel G. Krivitzky

2 Commander
Naval Surface Warfare Center
Indian Head Division
101 Strauss Avenue
Indian Head, MD 20640-5035
Attn.: C. F. Falkler/630
J. L. Barron

4 Commanding Officer
Naval Coastal Systems Station
NSWC Dahlgren Division
6703 West Highway 98
Panama City, FL 32407-7001
Attn.: Don Robeson/R05
D. Crute/R32
J. Rumbough
J. Mott

2 PEO Mine Warfare
PMS-407-DB
2531 Jefferson Davis Highway
Arlington, VA 22242-5167
Attn.: J. Johnson
Lt. Col. W. Hamm

1 Director, USMC Intel Activity
2033 Barnett Avenue
Quantico, VA 22134-5011
Attn.: M. Howard/MCIA12

4 Office of Naval Research
Ocean Atmosphere and Space Science
Technology Department (SMT)/322
800 N. Quincy Street
Arlington, VA 22217-5660
Attn.: R. Jacobson
D. Todoroff
K. Ward/335
T. Swean

1 Commander
Mine Warfare Command
325 Fifth Street SE
Corpus Christi, TX 78419-5032
Attn.: Code N 02

1 Mine Warfare EOD Branch
Pentagon Room 5E613
Washington, DC 20350-2000
Attn.: Major N. Tabbert

3 NVESD
Countermine Division
10221 Burbeck Rd., Suite 430
Ft. Belvoir, VA 22060-5806
Attn.: T. Broach
G. Law
J. Regnier

1 Naval Postgraduate School
1 University Circle
Monterey, CA 93943-5004
Attn.: Prof. X. Maruyama

2 Naval Facilities Engineering
Service Center
1100 23rd Avenue
Port Hueneme, CA 93043-4370
Attn: M. Fickel/ESC30
Maj. R. J. Lawson/MCLO

1 Presearch, Inc.
2361 Jefferson Davis Hywy/1200
Arlington, VA 22202
Attn: W. Ching

3 U.S. Army Engineering Center
320 Engineer Loop/166
Ft. Leonard Wood, MO 65473
Attn: Maj. Brian Baker
Col. C. M. Ferguson/TSM
Maj. J. S. Childress/TSM

2 U.S. Military Academy
West Point, New York 10996
Attn: LTC S. Ressler, Civil Engineering Department
CPT A. Alba, Department of Physics

1 Commanding Officer
MWSS-272
PSC 21032
Jacksonville, NC 28545-1032
Attn: LTC D. Brush

1 Commanding Officer
Naval EOD Technology Division
2008 Stump Neck Road
Indian Head, MD 20640-5070
Attn: Capt. Ted McCarley
Chris O'Donnell

1 U.S. Army Transportation School
Fort Eustis, VA 23604-5450
Attn: Maj. Michael B. Elko, USMC

1 USMC Engineer School
PSC Box 20069
Camp Lejuene, NC 28542
Attn: Maj. Charles Bridgeman

1 USMC CSS Enterprise NG
8th MT Bat
USMARFOR LANT
PCS Box 20132
Camp Lejuene, NC 28542-0132
Attn: MAJ James Flowers

1 U.S. Army DCSOPS-DAMO-FDZ
400 Army Pentagon/Rm 3C514
Washington, DC 20310-0460

1 MARCORSYSCOM CSLE-CE
2033 Barnett Avenue, Suite 315
Quantico, VA 22184
Attn: Lt. Col. William P. Macecevic Jr.

1 BG Robert Wilson, USA
Office of the Deputy CG
Rm 208, Gaffey Hall, Bldg. 2369
Old Ironsides Avenue
Ft. Knox, KY 40121

1 USA Soldier Systems Command
Natick RD&E Center
Natick, MA 01760-5019
Attn: R. M. Gonzalez/SSCNC-IM

1 AFR/MLQC
139 Barnes Dr./Suite 2
Tyndall AFB, FL 32403-5323
Attn: J. R. Porter

1 Lt(jg) John Simpson, CEC, USN
Third Naval Construction Brigade
258 Makalapa Dr.
Suite 200
Pearl Harbor, Hawaii 96860-7305

1 Capt. A. Woodfin, USMC
VMFA (AW) 225
MCAS Miramar
P.O. Box 452034
San Diego, CA 92145

1 Dept. of Naval Architecture and Ocean
Eng., U.S. Naval Academy
Annapolis, MD 21402

1 Joint Staff/J-4/RRD
The Pentagon, RM2D838
Washington, DC 20318-4000
Attn: Capt. P. Eltringham

1 Logistics Management Institute
2000 Corporate Ridge
McLean, VA 22102-7805
Attn: Mr. William Crowder

1 New Mexico Engineering Research Institute
1001 University Blvd. SE
Albuquerque, NM 87106-4342
Attn: Norman D. Falk

1 US TRANSCOM/TCJ5
508 Scott Drive
Scott AFB, IL 62225-5357
Attn: Mr. Keith Seaman

1 US TRANSCOM/TCJ3-0D
508 Scott Drive
Scott AFB, IL 62225-5357
Attn: Col (P) Charles W. Fletcher, Jr.

1 U.S. Army Combined Arms Support
Command
10500 A. Avenue
Fort Lee, VA 23801-6000
Attn: Ms. Katheryn M. O'Neill/ATCL-CBT

1 Commandant, US Army
Transportation School
Fort Eustis, VA 23604
Attn: BG William E. Mortenson

1 Army Management Staff College
5500 21st Street, Room 2607
Fort Belvoir, VA 22060-5934
Attn: Dr. Russell A. Vacante

1 Logistics Integration Agency
5001 Eisenhower Avenue
Alexandria, VA 22333
Attn: Mr. Robert Norton, Chief
Integration & Technology Division

1 Joint Staff/J-4/Mobility Division
The Pentagon/Room 2E827
Washington, DC 20318-4000
Attn: COL C. J. Evans, USAF

1 Air Combat Command ACC/LGX
130 Douglas Street, Suite 210
Langley AFB, VA 23665-2791
Attn: LTC Lawrence K. Grubbs

1 HQ, U.S. Marine Corps
Asst. Deputy COS for Installations and Log
2 Navy Annex
Washington, DC 20380-1775
Attn: Mr. Robert Hammond

1 Deputy Chief of Staff for Logistics
500 Army Pentagon
Room 1C565
Washington, DC 20310-0500
Attn: COL. William E. Wolf
Chief, Strategic Mobility Division

1 Applied Research Assoc.
P.O. Box 40128
104 Research Rd./Bldg. 9742
Tyndall AFB, FL 32403
Attn: Dr. Randy Brown

3 New Mexico Tech
EMRTC
Socorro, NM 87801
Attn: J. Cortez
T. Anderson
M. Banks

1 North Carolina Foam Industries
P.O. Box 1528
Mt. Airy, NC 27030
Attn: M. DeBone

2 General Plastics Mfg. Co.
P.O. Box 9097
Tacoma, WA 98409
Attn: Floyd Henry

1 Foamex International
1500 East 2nd Street
Eddystone, PA 14022
Attn: M. Hnatow

1 Gusmer Corporation
One Gusmer Drive
Lakewood, NJ 08701
Attn: Denis Commette
Doug Commette

1 Decker Industries, Inc.
P.O. Drawer "R"
Port Salerno, FL 34992
Attn: William Shaw

1 UCSC
1208 N. Grand
Roswell, NM 88201
Attn: Lela Wright
Jerry Whitaker

1 Futura Coatings, Inc.
9200 Latty Ave.
St. Louis, MO 63042, USA
Attn: Rodney D. Jarboe

1 SWD Urethane
P.O. Box 1422
Mesa, AZ 85211
Attn: Steve Hurd
Erich Robinson

1 IPI International, Inc.
7540 15th Street East
Sarasota, FL 34243
Attn: John A. Pardi

1 Transportation Engineering Agency
720 Thimble Shoals Blvd./Suite 130
Newport News, VA 23606-0276
Attn: B. A. Hines

1 Joint Mission Analysis Group
Johns Hopkins University/APL
11100 Johns Hopkins Rd.
Laurel, MD 20723-6099
Attn: George W. Pollit

1 DERA Bincleaves
Newtons Road
Weymouth, Dorsett DT4 8UR, U.K.
Attn: Stephen R. Takel

1 Engineer and NBC Defense School
Farum Barracks
DK-3520 Farum
Denmark
Attn: Maj. L. R. Schmidt

1 ARA
4300 San Mateo Blvd. N.E.
Albuquerque, NM 87110
Attn: J. Bratton

1 Vernon Joynt
P.O. Box 912454
2396 Mundt St. Watloo
Pretoria, Silverton 0127
South Africa

1 IAI-RAMTA Division
Beer Sheva
P.O. Box 323
Israel 84102
Attn: Zeev Scheiring

1 Hardinge Engineering Co.
2032 Bamboo Drive
Lexington, KY 40503
Attn: B. C. Hardinge

1 University of Western Australia
Dept. of Mech. & Materials Engineering
Nedlands
West Australia 6907
Professor James Trevelyan

1 MgM
Diessemer Bruch 150
47805 Krefeld
Germany
Attn: Hendrik Ehlers, Dir.

1 Director, Technology Programs
Lockheed Martin Government
Electronic Systems
199 Borton Landing Road
P.O. Box 1027
Moorestown, NJ 08057-0927
Attn: David A. Philips

1 Lockheed Martin Tactical
Aircraft Systems
P.O. Box 748, MZ-1225
Fort Worth, TX 76101-0748
Attn: Steven K. Saiget

1 Defense Science and Technology Org.
Aeronautical and Maritime Research
Laboratory
P.O. Box 4331 Melbourne 3001
Attn: Roy Bird

1 Stanley Corporation
300 North Washington Street
Suite 400
Alexandria, VA 22314
Attn: Ed Savacool

3 Defense Material Organization
Ministry of Defense
Depot Road #18-05
Defense Technology Tower A Singapore
109679
Attn: Dr. Terence Goh
Tan Kat Chui
Lim Yoke Beng

1 American Systems Corporation
Joint Non-Lethal Weapons Programs
241 South Fraley Blvd., Suite 100
Dumfries, VA 22026
Attn: A. J. Kessel

1 Applied Research Laboratory
The Pennsylvania State University
P.O. Box 30
State College, PA 16804-0030
Attn: Nicholas C. Nicholas, Ph.D.

1 Menlo Logistics
2000 St. James Place
Houston, TX 77056
Attn: Mark F. Morris

1 Global Landmine Survey
2001 S. Street NW, Suite 310
Washington, DC 20009, USA
Attn: Sayed Aqa

1 Humanitarian Demining Center
James Madison University
College of Integrated Science and Technology
Harrisonburg, VA 22807
Attn: Dennis C. Barlow

1 E. Allan Blair
4540 E. Flint Wood
Flagstaff, AZ 86004

1 Gerard Tan
21, Tan Quee Lan Street,
#01-03A Heritage Place
Singapore 188108

1 Army Program Manager
American Embassy – Singapore
PSC 470, Box ODC
FPO AP 96507
Attn: Major David Hyres

1 LCDR John P. Stokely, USN
CNO Strategic Studies Group
Naval War College
686 Cushing Road
Newport, RI 02841-1207

1 United Methodist Church
Room 1359
475 Riverside Dr.
New York, NY 10115
Attn: James Gulley
Executive Secretary

1 Texas A&M University
Dept. Electrical Engineering
College Station, TX 77843-3128
Attn: Robert D. Nevels

1 Strategic Technologies, Inc.
6121 Indian School Rd. NE, Suite 234
Albuquerque, NM 87110
Attn: Robert J. Malins
Technical Director

2 Los Alamos Technical Associates, Inc.
2400 Louisiana Blvd., NE
Bldg. 1, Suite 400
Albuquerque, NM 87110
Attn: C. O. Schmidt

	MS 0367	J. H. Aubert, 1811
10	MS 0783	S. H. Scott, 5832
	MS 0634	B. J. Gomez, 12351
20	MS 0775	L. S. Roach, 5316
	MS 1221	D. M. Rondeau, 15003
	MS 0860	B. G. Hance, 2618
	MS 0367	P. B. Rand, 1811
	MS 1452	J. A. Merson, 2552
10	MS 1452	R. L. Woodfin, 2552
	MS 1454	M. G. Vigil, 2554
	MS 1454	D. E. Paul, 2554
	MS 1454	R. A. Benham, 2553
	MS 1156	P. W. Cooper, 15322
	MS 9018	Central Technical Files 8940-2
2	MS 0899	Technical Library, 9616
	MS 0612	Review & Approval Desk, 9612 For DOE/OSTI